TRANSVERSE WAKEFIELD ANALYSIS FOR THE NLC & JLC DETUNED STRUCTURES ON A PARALLEL COMPUTER *

Xiaowei Zhan and Kwok Ko†
SCCM Program, Stanford University, Stanford, CA 94305
† Stanford Linear Accelerator Center, Stanford University, Stanford, CA 94309

Abstract

The detuned structure (DS) has been proposed as one possible design to control the emittance growth of long bunch trains in linear colliders due to transverse wakefields. A DS typically consists of over a hundred cells with tapering from cell to cell of the order of few microns to decohere the dipole modes. The design parameters are targeted for two orders of magnitude reduction in the wakefield experienced by the trailing bunch. Field analysis of such a large heterogeneous structure is impractical with finite-difference schemes using structured grids. This paper presents the results from calculations performed on a parallel computer using a finite-element code based on an unstructured grid. We discuss the parallel implementation issues and show comparisons between simulation results and the wakefield data taken on both the NLC and JLC detuned structures.

1 INTRODUCTION

As all linear collider designs adopt acceleration of long bunch trains to increase luminosity the dilution of the beam emittance due to wakefield effects in the linac is an important problem to overcome in accelerator structure design. The detuned structure (DS) is considered as one viable option to suppress the long range wakefields that lead to cumulative beam break-up instability. In the DS the cell dimensions are tapered to provide a Gaussian distribution of the most harmful dipole modes so that their detuning results in a substantial decrease in the wakefield experienced by the trailing bunches. Both SLAC and KEK have a DS design for their proposed X-Band linear colliders (NLC and JLC). Fig. 1 (a) shows the cell geometry in a typical DS. The unit cell is formed between disks whose aperture a and thickness t vary along the structure according to the distributions shown in Fig. 1 (b). The tapering profile for a is to Gaussian detune the 1st dipole band while that for t applies to the higher bands (3rd and 6th). The cell radius b is then adjusted to tune the accelerating mode to 11.424 GHz at 120 degree phase advance across the cell length L.

2 FINITE ELEMENT WAKEFIELD ANALYSIS

Many wakefield calculations have been carried out to assess the effectiveness of the DS in wakefield reduction. But they have all been based on approximate methods because the size of the problem precludes a direct numerical approach until now. Also, previous analysis have mostly simplified the cell geometry so that ends of the disks are treated as flat than round. The methods used include equivalent-circuits [1], mode-matching [6], and the open-mode [5] expansion. Generally the wakefield results obtained from these studies agree qualitatively with measurements. Nevertheless it is of interest to obtain the wakefield from a direct simulation of the DS on a numerical grid that models closely the exact geometry and dimensions.

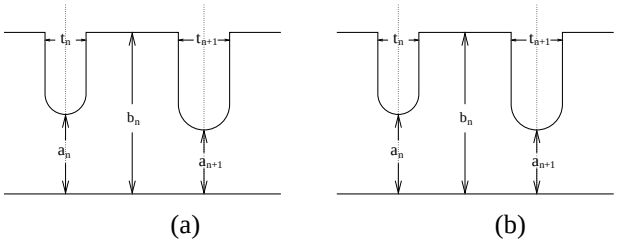

Figure 1: (a) The dimensions of a typical cell; (b) Variations of cell dimensions.

There are difficulties in applying numerical field solvers to the DS geometry especially if they are of the finite-difference (FD) type that employs a structured grid. First, to fit the gradual taper in a and b would require mesh sizes so small that the mesh becomes prohibitively large to be practical to simulate on any computer. One can exploit grading of the mesh sizes (non-uniform mesh) to reduce the number of mesh points. But over grading can lead to mesh cells with such disparate dimensions that convergence may become an issue for the solver. Also, structured grids are not capable of modeling curved boundaries accurately. Diagonal mesh can help to provide a better fit but the unusually large aspect ratio can cause the solution matrix to be ill-conditioned.

The finite-element (FE) method has been shown to be highly accurate and efficient in modeling accelerator structures [4]. The FE unstructured grid is able to fit small differences in geometry and to refine locally around curved boundaries without significant increase in the global number of elements or degrees of freedom (DOF). The DOF's can be further minimized without loss in accuracy through the use of higher-order elements. These improvements altogether are still not sufficient to reduce the problem size enough for the simulation to be practical on any high-end workstation. It becomes apparent that more efficient gridding (adaptive mesh refinement) and more powerful computing resources (parallel processing) are needed.

3 ADAPTIVE MESH REFINEMENT

In finite element analysis, the accuracy of the solution improves as the mesh is refined. The simplest refinement is

* Work supported by the Department of Energy, contract DE-AC03-76SF00515.

0-7803-4376-X/98/$10.00 © 1998 IEEE

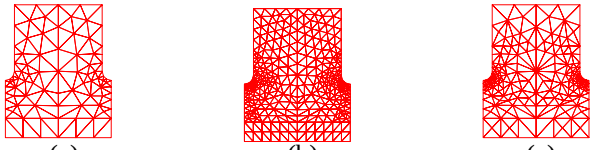

(a) (b) (c)

Figure 2: (a) Initial mesh; (b) Uniform refinement; (c) Adaptive refinement.

to subdivide each element over the entire mesh so the increase in DOFs scales with the number of subdivisions. A more cost effective way is to refine adaptively to keep the number of extraneous DOFs to a minimum. We use the local integral of the energy density gradient as a criteria to determine if local refinement is necessary, and stop the refinement when a specified tolerance is reached. This indicator turns out to be very effective from our numerical experiments in approximating the optimal mesh for a desired accuracy. Fig. 2 show an initial mesh, a uniformly refined mesh, and an adaptively refined mesh. The two refined meshes yield the same accuracy but the adaptively refined mesh has half the number of DOFs, thereby producing a significant savings in memory requirement and run time.

4 PARALLEL IMPLEMENTATION

The DS geometry is highly amenable to domain decomposition for parallel processing because the partitioning is straightforward. Each cell in the long structure is assigned a processing node. In the single program multiple data (SPMD) model, global data such as meshes and matrices are distributed to the nodes where global operations can be processed locally. As shown previously in Fig. 1 the cell is bounded by half-disks (subdomain) so that sharing of data between nodes is limited to the field quantities at the cell apertures. This way the communication between nodes is kept to a minimum, and is achieved using the message passing interface (MPI).

The discretization of the Maxwell's equations in the frequency domain by FE results in a generalized eigenvalue problem, $Kx = \lambda Mx$. Both M and K are large, sparse and symmetric while M is positive definite. We use the Lanczos algorithm in the solver for its superior convergence properties which is ideal for computing extremal eigenvalues of large problems [3]. With the shift-invert technique, in each Lanczos iteration one solves the linear system $\tilde{K}x = b$, where $\tilde{K} = K - \sigma M$, and σ is the shift introduced to accelerate convergence by better separating the eigenvalues. Since solving the linear system constitutes the most time-consuming operation in the entire program, its parallel implementation is important for high parallel efficiency.

One way to look at the linear system under the domain decomposition introduced earlier is to separate the DOFs into "interior" ones that reside inside a subdomain (cell) and "interface" ones that are shared by the neighboring subdomains. Since there is no coupling between the "interior" DOFs from different subdomains, and the "interface" DOFs are far less in number, $\tilde{K}$ can be reordered in the form

$$\tilde{K} = \begin{pmatrix} A & C^T \\ C & F \end{pmatrix},$$

where A is a block diagonal matrix with the ith diagonal block A_i resulted from the "interior" DOFs in the ith subdomain, while F consists of only the "interface" DOFs, and C provides the coupling between them.

The next step is to decompose the matrix $\tilde{K}$ as

$$\tilde{K} = \begin{pmatrix} I & 0 \\ CA^{-1} & I \end{pmatrix} \begin{pmatrix} A & C^H \\ 0 & G \end{pmatrix} \tag{1}$$

where $G := F - CA^{-1}C^H$ is the Schur complement [2].

Now, since A is block diagonal, $A^{-1}v$ can be computed in parallel without interprocessor communication.

Because the size of G is relatively small, and it is block tridiagonal, the communication overhead to form it to explicitly is not significant. Hence, through the decomposition (1), the linear system $\tilde{K}x = b$ can be solved efficiently in parallel.

The block decomposition (1) is particularly useful and flexible for providing a framework for parallel implementation of the linear solvers. It allows us to achieve the parallelism for solving the global linear system regardless of how the local linear systems are solved.

5 TRANSVERSE WAKEFIELDS IN THE NLC & JLC

One concern over the stability of long bunch trains in next generation linear colliders such as the NLC and the JLC is the deflection of the beam due to long-range transverse wakefields. The wakefield at distances of the order of the bunch spacing is mainly due to the resonant modes of the structure, and in the transverse case, is given by

$$W(s) = \frac{2}{N_c} \sum_{i=1}^{N} K_i \sin(\frac{\omega_i s}{c}) \tag{2}$$

where ω_i, K_i are the frequency and the kick factor of mode i respectively, N is number of modes excited by the bunch and N_c is the number of cells in the structure. The kick factor is determined from the synchronous voltage

$$V_i = \int_{z_{min}}^{z_{max}} E_z(r_o, z)\ \exp{(j\frac{\omega_i}{c}z)}dz$$

and the stored energy

$$U_i = \frac{1}{2}\epsilon \int |E|^2\ dV + \frac{\mu^{-1}}{2} \int |B|^2\ dV$$

via the expression

$$K_i = \frac{|V_i|^2}{4(\omega_i/c)U_i\ r_o^2\ L}$$

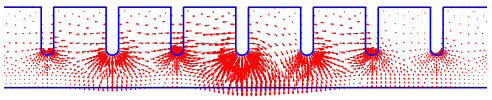

Figure 3: E-field (cell 163–170) of mode 166 for NLC DS.

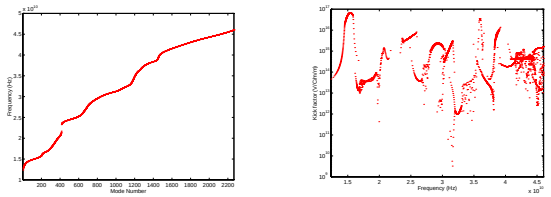

(a) (b)

Figure 4: Dipole modes for NLC: (a) frequency vs mode number; (b) kickfactor vs frequency.

Except for the open-mode method, other wakefield calculations have included only modes from the first two dipole bands although it is recognized that contributions from higher bands can be important as well. The open-mode analysis extends to the higher bands but thus far has considered only flat-ended disks in the cell geometry. The present work takes into account the exact cell geometry and includes as many higher band contributions as computation time would allow.

6 SIMULATION RESULTS

We have developed a new FE field solver using quadratic elements and including both parallelization and adaptive refinement features. Written in C++, the program is modular in structure and is compatible with any mesh generator. We used MODULEF to generate the mesh data for the NLC and JLC DS geometries. The program has been running on the Intel's Paragon XP/S 150 at Oak Ridge National Laboratory. This massively parallel computer has 1,024 nodes with two 75-MFLOPS i860 XP processors and 64 MBytes memory per node. Based on the one cell per node strategy described earlier, it is clear that memory rather than CPU is the limiting factor in our simulations.

The NLC X-Band DS is 1.8m long consisting of 206 cells and Fig. 3 shows the 166th mode in the first dipole band that is localized between cell 163 and 170 in that structure. We have computed the contributions from eleven bands for a total of 2266 modes with wall loss included. Figs. 4 show the frequencies of these modes and their kick-factors. Applying these data to the wakefield in (2) results in Fig. 5. Also shown are the measured data and the calculated result from equivalent circuit method. For the 150 cell JLC DS, we computed 1466 modes and the comparison between finite-element, measurement, and open-mode results is displayed in Fig. 6. Both the NLC and JLC wakefield analysis indicate a closer agreement between the finite-element result and measured data.

7 SUMMARY

This paper reports the first-ever direct field analysis of the transverse modes in a long tapered structure with realistic geometries and dimensions. The enabling capability is a new finite-element program that utilizes higher-order elements, adaptive refinement and parallel processing. The cpu time required for the NLC and JLC detuned structure calculations is in the ten's of hours even when contributions from thousands of modes are considered. In terms of parallel computing efficiency the speedup increase is close to linear. They lend support to our assertion that parallel computing is practical for accurately analyzing large heterogeneous systems.

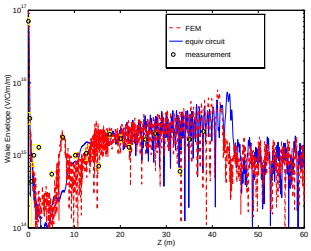

Figure 5: For NLC: Wake envelope comparison between FEM and equivalent circuit method; the circles are measured data.

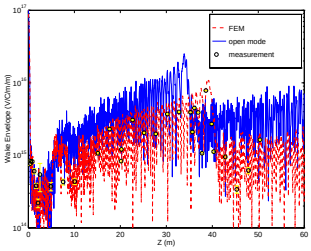

Figure 6: For JLC: Wake envelope comparison between FEM and open-mode method; the circles are measured data.

8 ACKNOWLEDGMENTS

We are grateful to Drs. Cho Ng, Zenghai Li and Vinay Srivinas for their generous help and fruitful discussions. We'd like to thank Profs. Roger Miller and Gene Golub for their interests in the problem. We also acknowledge the use of Intel Paragons located in ORNL's CCS.

9 REFERENCES

[1] K. L. F. Bane and R. L. Gluckstern, *The transverse wakefields of a detuned X-band accelerator structure*, SLAC-PUB-5783, 1992.

[2] G.H. Golub and C.F. Van Loan, *Matrix Computations*, The John Hopkins University Press, Baltimore, 3rd edition, 1996.

[3] Y. Saad, *On the Rates of Convergence of the Lanczos and the Block Lanczos Methods*, SIAM J. Num. Anal. 17, 687-706, 1980.

[4] Eric Nelson, SLAC Report 92-16, 1992.

[5] M. Yamamoto, *Study of Long-Range Wake Field in Accelerating Structure of Linac*, KEK Report 94-9, 1995.

[6] S. A. Heifets and S. A. Kheifets, *Coupling impedance for modern accelerators*, AIP 249, 1992, pp. 151-235.